Journal of Magnetics 4(2), 60-64 (1999)

The Effect of Additive Co on the Magnetic Properties of $Fe_3B/Nd_2Fe_{14}B$ Magnets

Choong Jin Yang, Eoun Byung Park, Yong Soon Hwang[1] and Eng Chan Kim[1]

Electromagnetic Materials Lab., Research Institute of Industrial Science & Technology(RIST), P.O. Box 135, Pohang 790-600, Korea
[1]Dept. of Physics, Youngnam National University, Kyungsan 214-1, Kyungbook, Korea

(Received 10 May 1999)

The addition of Co into $Nd_4Fe_{77.5-x}Co_x(HfGa)_yB_{18.5}$($0 \leq x \leq 5$, y=0, 0.5) was found to enhance the magnetic properties of $Fe_3B/Nd_2Fe_{14}B$ nanocomposite magnets. The enhancement resulted from the fact that Co retarded the crystallization of α-Fe or Fe_3B but accelerated that of $Nd_2Fe_{14}B$. The decreased interval between the onset of crystallization temperature of Fe_3B and $Nd_2Fe_{14}B$ phases enabled the grain growth of each phase to be uniform during a post annealing of the melt spun ribbons. The addition of 3~5 at.% Co into ternary composition $Nd_4Fe_{77.5}B_{18.5}$ increased the coercivity ($_iH_c$) from 3.27 to 3.54 kOe with the enhanced remanence value ($4\pi M_r$) around 11.54 kG. From the ribbon magnets of $Nd_4Fe_{71.5}Co_5Hf_{0.5}Ga_{0.5}B_{18.5}$ made at 26 m/sec and annealed at 680 °C for 10 min, the magnetic properties of B_r=11.54 kG, $_iH_c$=3.54 kOe, and $(BH)_{max}$=14.35 MGOe were obtained from volume production line.

1. Introduction

Recently, Yang *et al.* [1] introduced an external magnetic treatment to enhance the reduced remanence (M_r/M_s) value up to 0.84 in the $Fe_3B/Nd_2Fe_{14}B$ nanocomposite magnets containing Ga and Hf. However, $Fe_3B/Nd_2Fe_{14}B$ nanocomposite magnets prepared from NdFeGaHfB system did not show a strong enough coercivity ($_iH_c$). Because the intrinsic coercivity was reduced as a result of the exchange interaction and particularly in the presence of large volume of α-Fe.

It is well established that the partial substitution of Fe by Co substantially enhances the saturation magnetization of (Fe, Co) solid solution and $Nd_2(Fe, Co)_{14}B$ phase [2, 3]. Similarly, one could expect a higher B_r and $(BH)_{max}$ from Co-containing nanocomposites. Since the addition of Co may also change the viscosity of liquid phase, the characteristics of melt spun alloys could be altered in terms of crystallization behavior. Recently, some work dealt with the $Nd_2Fe_{14}B$/α-Fe base nanocomposites were reported by Davis *et al.* [4]. The reports claimed that the partial substitution of Fe by Co increases Curie temperature, and hence the thermal stability. However, both the B_r and $(BH)_{max}$ were not reported to be significantly affected by the substitution in the melt-spun alloys.

Magnetic properties of the nanocomposites are influenced sensitively by their microstructures such as the volume ratio between hard and soft phases, the grain size, and their uniform distribution [5]. Since the order of formation and the growth rate of each phase, $Nd_2Fe_{14}B$, Fe_3B and α-Fe are different, the effect of additives such as Co must be clarified. In this study, therefore, the addition of Co into $Nd_2Fe_{14}B/Fe_3B$ base nanocomposites are reported.

2. Experiment

The ingots of $Nd_4(Fe_{77.5-x}Co_x)(Hf, Ga)_yB_{18.5}$ ($0 \leq x \leq 5$, y=0, 0.5) were prepared using metals in purity of Nd 99 wt.%, FeB alloy (B 13 wt.%), Ga 99.5 wt.%, Hf 99.5 wt.% and Co 99.5 wt.%, respectively. These ingots were initially alloyed by arc melting for several times to obtain homogeneous composition, and then melt spun at a wheel speed of 26 m/sec. The magnetic phases were identified by XRD analysis, and thermal behaviors were examined using DTA and TMA in the temperature range up to 850 °C. On the basis of DTA data, the melt spun materials were annealed at 620~760 °C for 10 minutes without an external magnetic field. Magnetic properties were characterized using a vibrating sample magnetometer applying an appropriate demagnetization factor. Microstructure was examined using a high resolution transmission electron microscope. An exact composition was identified by ICP analysis.

3. Results and Discussion

3.1. Magnetic properties

For the nanocomposite magnets exchange coupling interaction is sensitively dependent upon if a grain boundary phase is present or not. Therefore a precise control of desired composition is required to avoid the formation of

harmful grain boundary phase. By utilizing ICP analysis it was possible to control the elemental contents in an accuracy of –4%~+1.0 wt.% for Nd, 0.5~2.8 wt.% for B, and –0.66~+0.88 wt.% for Co with respect to the required composition on the basis of theoretical density. The as-spun ribbons of $Nd_4(Fe_{77.5-x}Co_x)$ (Ga, Hf)$_yB_{18.5}$ ($0 \leq x \leq 5$, $0 \leq y \leq 0.5$) made at a wheel speed faster than 26 m/sec were always complete amorphous. However, the free surface of the ribbons quenched at the wheel speed slower than 26 m/sec contained Fe_3B phase in the as-spun state. Therefore the wheel speed faster than 26 m/sec was a prerequisite for obtaining a fine grain structure from the amorphous material.

XRD patterns for ternary composition $Nd_4Fe_{77.5}B_{18.5}$, and Co containing $Nd_4Fe_{71.5}Co_5Hf_{0.5}Ga_{0.5}B_{18.5}$ ribbons, both annealed at 680 °C for 10 minutes, shown in Fig. 1 indicate very small amount of α-Fe formation, but no clear difference in the reflection spectrum. Therefore Co and Ga/Hf are believed to substitute into $Nd_2Fe_{14}B$ crystal after annealing. However, the substitution behavior of each Co, Ga/Hf atoms during crystallization of the nanoscaled α-Fe, Fe_3B and $Nd_2Fe_{14}B$ is different. Since the initial formation of α-Fe/Fe_3B at around 600 °C is followed by $Nd_2Fe_{14}B$ [6] from the amorphous matrix, Co would be piled up first at the

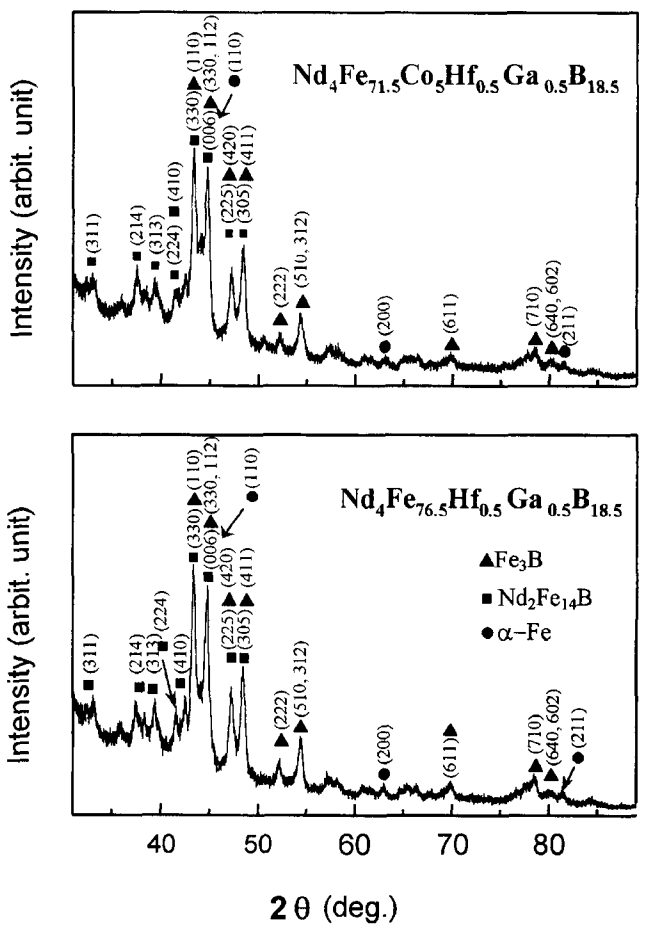

Fig. 1. XRD patterns of $Nd_4Fe_{76.5}Hf_{0.5}Ga_{0.5}B_{18.5}$ and $Nd_4Fe_{71.5}Co_5Hf_{0.5}Ga_{0.5}B_{18.5}$ ribbons after annealing at 680 °C for 10 min.

Table 1. Result of fitted lattice constants of $Nd_2(Fe,Co)_{14}B$ and Fe_3B phases

Alloy composition	$Nd_2Fe_{14}B$ (tetragonal)		Fe_3B (tetragonal)	
	a (Å)	c (Å)	a (Å)	c (Å)
$Nd_4Fe_{76.5}Hf_{0.5}Ga_{0.5}B_{18.5}$	8.812	12.180	8.634	4.306
$Nd_4Fe_{73.5}Co_3Hf_{0.5}Ga_{0.5}B_{18.5}$	8.793	12.125	8.618	4.291
$Nd_4Fe_{71.5}Co_5Hf_{0.5}Ga_{0.5}B_{18.5}$	8.783	12.108	8.617	4.290

interfaces of α-Fe/Fe_3B/amorphous. Accordingly fine grained α-Fe/Fe_3B is expectable due to the slow growth. At the same time Ga/Hf atoms are believed to control the grain growth of $Nd_2Fe_{14}B$ which is formed at the later stage of nanocomposite crystallization [6]. From an elaborate curve fitting method of XRD patterns, the changes in lattice parameter resulted from the addition of Co into $Nd_4Fe_{76.5}Hf_{0.5}Ga_{0.5}B_{18.5}$ were obtained as shown in Table 1. The lattice parameters for both of the $Nd_2Fe_{14}B$ and Fe_3B, especially *c* parameter of $Nd_2Fe_{14}B$ lattice, were observed to decrease obviously by the increase of Co.

Fig. 2 shows the effect of Co addition on the crystallization behavior for Co-free and Co-containing $Nd_4Fe_{76.5}Ga_{0.5}Hf_{0.5}B_{18.5}$ alloys. The addition of 5 at.% Co was observed to increase the crystallization temperature (T_x) of Fe_3B from 598 to 608 °C, but decrease that of $Nd_2Fe_{14}B$ from 642 to 635 °C, respectively. It is of interesting to note that the gradual increase of Co addition into $Nd_4Fe_{76.5}Ga_{0.5}Hf_{0.5}B_{18.5}$ by 3, 4 and 5 at.%, the interval between the crystallization temperature of the Fe_3B and $Nd_2Fe_{14}B$ phases was measured to get closer. Therefore the closer crystallization temperatures might make Fe_3B and $Nd_2(Fe, Co)_{14}B$ phase have a uniform size distribution after the complete transformation during annealing. Even the small addition of Co was also found to increase the Curie temperature (T_c) of each phase. The observed T_x and T_c are summarized in Table 2.

Taking into account the increase in T_c for Fe_3B phase, however, the substitution of Co into Fe_3B should not be

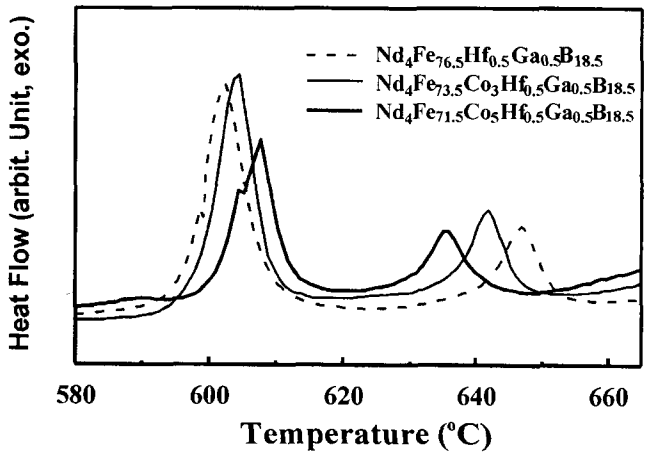

Fig. 2. DTA curves of $Nd_4Fe_{76.5-x}Co_xHf_{0.5}Ga_{0.5}B_{18.5}$ ribbons melt spun at 26 m/sec.

Table 2. The variarion of Curie and crystallization temperature by the addition of Co

Composition	T_c (°C)			T_x (°C)	
	$Nd_2Fe_{14}B$	Fe_3B	α-Fe	$Nd_2Fe_{14}B$	Fe_3B
$Nd_4Fe_{76.5}Ga_{0.5}Hf_{0.5}B_{18.5}$	340	510	750	646	598
$Nd_4Fe_{73.5}Co_3Hf_{0.5}Ga_{0.5}B_{18.5}$	355	525	800	641	599
$Nd_4Fe_{72.5}Co_4Hf_{0.5}Ga_{0.5}B_{18.5}$	355	530	830	638	603
$Nd_4Fe_{71.5}Co_5Hf_{0.5}Ga_{0.5}B_{18.5}$	360	550	830	635	608

overlooked.

Fig. 3 shows high resolution TEM micrographs showing the grain aspect of $Nd_4Fe_{76.5}Ga_{0.5}Hf_{0.5}B_{18.5}$ and $Nd_4Fe_{71.5}Co_5Ga_{0.5}Hf_{0.5}B_{18.5}$ ribbons both annealed at 680 °C for 10 minutes. It was very difficult to find an obvious difference in grain boundary aspect except that the uniform grain distribution was observable for the Co-containing alloys. Because all the grains of nanoscaled Fe_3B and $Nd_2Fe_{14}B$ were crystallized coherently without a boundary phase from the amorphous matrix. However, the overall grain size of Co-containing alloys was found to decrease gradually by

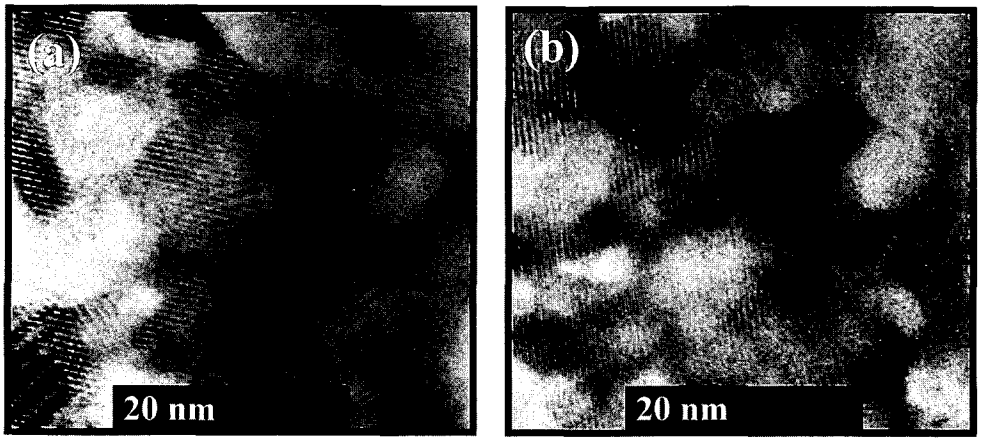

Fig. 3. High resolution TEM microgarphs showing the grain aspect of (a) $Nd_4Fe_{76.5}Hf_{0.5}Ga_{0.5}B_{18.5}$ and (b) $Nd_4Fe_{71.5}Co_5Hf_{0.5}Ga_{0.5}B_{18.5}$ ribbons both annealed at 680 °C for 10 min.

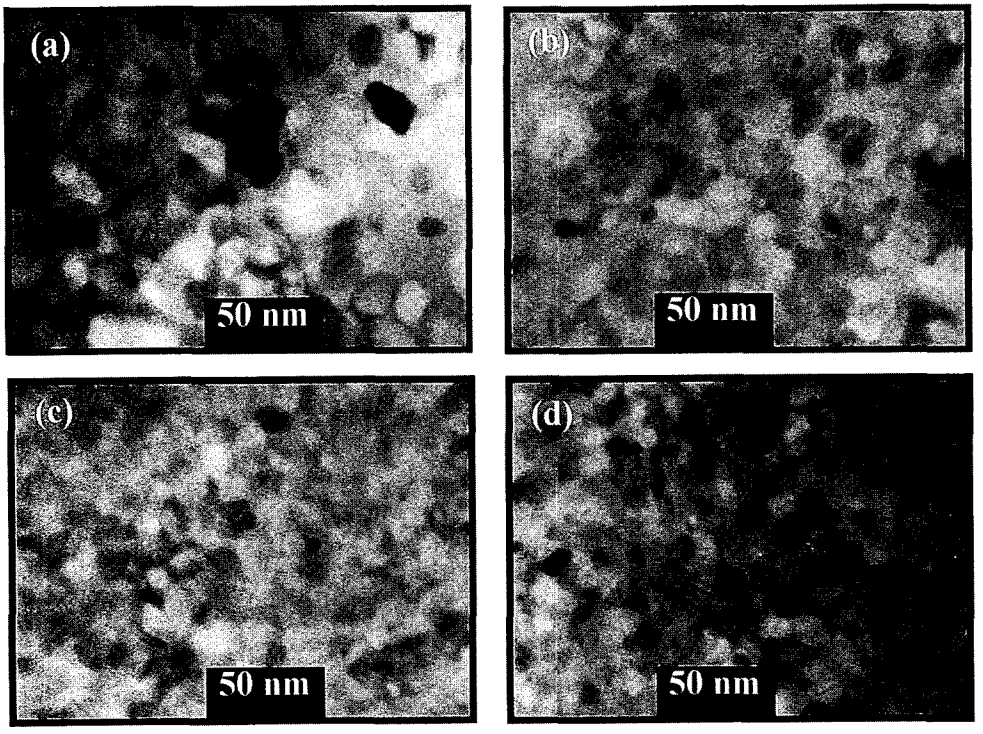

Fig. 4. High resolution TEM maicrographs showing the grain size distribution as a function of Co addition; (a) $Nd_4Fe_{77.5}$-$B_{18.5}$, (b) $Nd_4Fe_{76.5}Hf_{0.5}Ga_{0.5}B_{18.5}$, (c) $Nd_4Fe_{73.5}Co_3Hf_{0.5}Ga_{0.5}$-$B_{18.5}$, and (d) $Nd_4Fe_{71.5}Co_5Hf_{0.5}Ga_{0.5}B_{18.5}$ ribbons. All were annealed at 680 °C for 10 min.

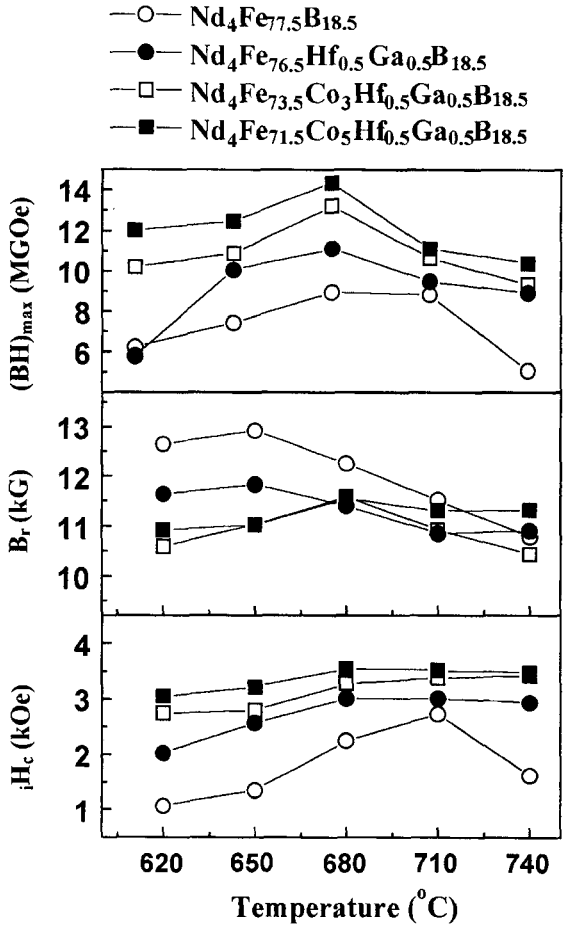

Fig. 5. Magnetic properties of $Nd_4Fe_{76.5-x}Co_xHf_{0.5}Ga_{0.5}B_{18.5}$ ribbons melt spun at a wheel speed of 26 m/sec as a function of annealing temperature.

the increase of Co addition from 3 to 5 at.% as shown in Fig. 4. The grain size of $Nd_4Fe_{76.5}Ga_{0.5}Hf_{0.5}B_{18.5}$ was found to be in the range of 10~25 nm while that of the $Nd_4Fe_{71.5}Co_5Ga_{0.5}Hf_{0.5}B_{18.5}$ was in the range of 10~20 nm which is quite narrow size distribution.

The principal magnetic properties of the Co-containing alloys are plotted as a function of annealing temperature in Fig. 5. Basically the maximum coercivity ($_iH_c$) values for both the ternary composition ($Nd_4Fe_{77.5}B_{18.5}$) and Co-containing alloys are obtained around at 680~710 °C. The previous study [5] on NdFeCoGaHfB alloys containing 3 at.% Co reported that the maximum coercivity was obtained from the samples having the average grain size of 22 nm. In this sense one can assure that the critical grain size for the $Nd_4Fe_{77.5}B_{18.5}$ alloy is formed at about 710 °C where the maximum coercivity is obtained. By the addition of Co from 3 to 5 at.%, however, the maximum coercivity can be seen to occur at a lower annealing temperature with a much higher values than that of the ternary composition. Also, as Yang *et al.* pointed out [5], the maximum remanences for these $Fe_3B/Nd_2Fe_{14}B$ nanocomposites always take place at much lower the temperature than the temperature where the maximum coercivity is obtained. Accordingly, the highest

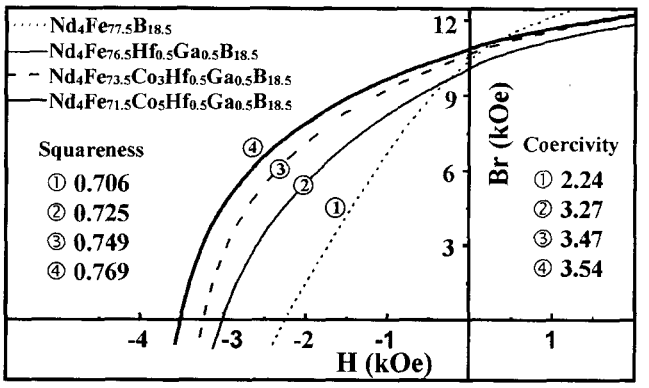

Fig. 6. Demagnetization curves of $Nd_4Fe_{76.5-x}Co_xHf_{0.5}Ga_{0.5}B_{18.5}$ melt spun ribbons annealed at 680 °C for 10 min.

$(BH)_{max}$ for these Co-containing alloys are obtained at 680 °C for 10 minutes. The highest $(BH)_{max}$ was 14.35 MGOe obtained from the $Nd_4Fe_{71.5}Co_5Ga_{0.5}Hf_{0.5}B_{18.5}$ alloy.

More detailed demagnetization curves of nanocomposite alloys containing different amount of Co are shown in Fig. 6. All the ribbon samples were annealed at 680 °C for 10 minutes. The curve of ternary composition $Nd_4Fe_{77.5}B_{18.5}$ indicates the mixture of amorphous and nanoscaled magnetic phases, *i.e.*, $Fe_3B/Nd_2Fe_{14}B$ which results in a constriction along the demagnetization curve. The annealing treatment at 680 °C for 10 minutes for this alloy probably provides the grains under the critical size. If Co is added into the ternary composition the squareness of the curves improves prominently. The Co addition from 3 to 5 at.% increases the coercivity from 3.27 to 3.54 kOe with the enhanced remanence value about 11.54 kG. This improved suqareness of demagnetization curves of Co-containing alloys indicates that phase separation of Fe_3B and $Nd_2(FeCo)_{14}B$ from the amorphous matrix activated the exchange coupling between those grains due to slow growth rate of Fe_3B/α-Fe and fine grains of $Nd_2Fe_{14}B$. The resultant remanence (B_r) and coercivity ($_iH_c$) were 11.54 kG and 3.54 kOe, respectively.

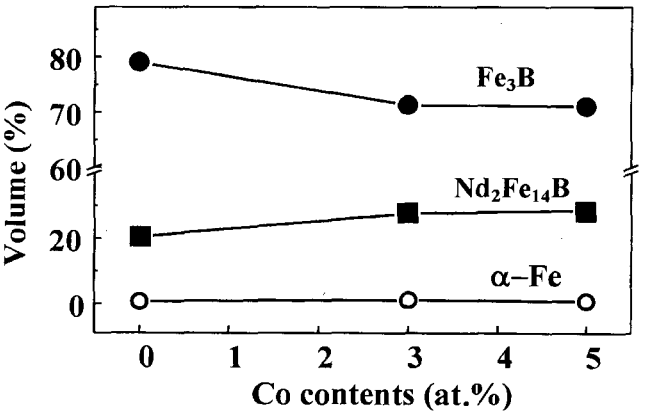

Fig. 7. Variation of volume fraction of two phases in $Nd_4Fe_{76.5-x}Co_xHf_{0.5}Ga_{0.5}B_{18.5}$ ribbons as a function of Co addition (x=0, 3, and 5)

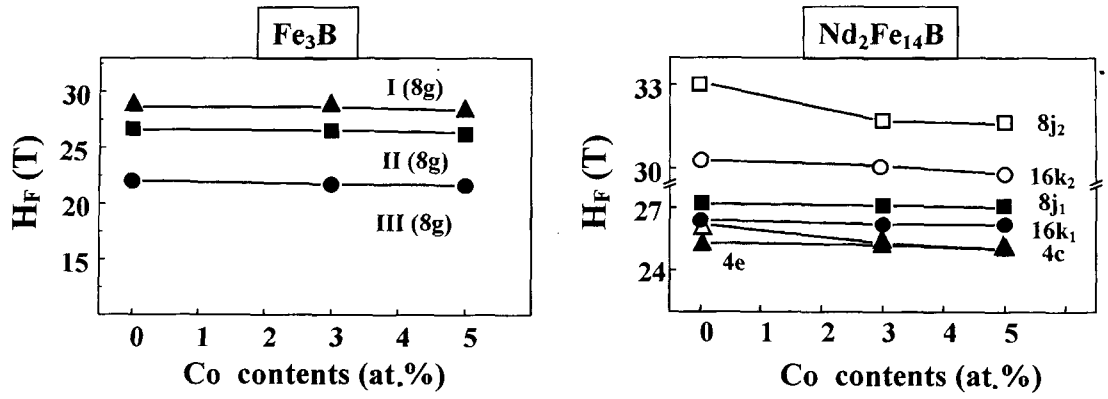

Fig. 8. Variation of hyperfine field(HF) of Fe_3B and $Nd_2Fe_{14}B$ phases in $Nd_4Fe_{76.5-x}Co_xHf_{0.5}Ga_{0.5}B_{18.5}$ ribbons as a function of Co addition (x=0, 3, and 5).

3.2. The result of Mossbauer spectroscopies

In order to clarify the effect of Co addition into the ternary composition $Nd_4Fe_{77.5}B_{18.5}$, Mossbauer spectroscopy was carried out for each alloy containing 3, 4 and 5 at.%, respectively. The concerns were focused on the effects of Co in terms of respective volume fraction of Fe_3B and $Nd_2Fe_{14}B$ phase, and the variation of hyperfine field (HF) of the nonequivalent Fe sites for each Fe_3B and $Nd_2Fe_{14}B$ crystal where Co atoms are supposed to substitute the Fe atoms. Fig. 7 shows the variation of volume fraction for each Fe_3B and $Nd_2Fe_{14}B$ formed after annealing the $Nd_4Fe_{76.5-x}Co_xHf_{0.5}Ga_{0.5}$ alloys at 680 °C for 10 minutes. The volume fraction of Fe_3B was found to be about 71% which was not varied with increasing the Co content up to 5 at.%. The presence of α-Fe was found to be around only 1 vol. % as was suggested in the XRD pattern in Fig. 1. The volume fraction of $Nd_2Fe_{14}B$ phase was observed to be about 29% for the treatment in this study.

Fig. 8 shows the variation of hyperfine field (HF) as a function of Co addition. Three ineuqivalent Fe sites of Fe_3B and six ineuqivalent Fe sites of $Nd_2Fe_{14}B$ were analyzed with increasing the Co content. Basically no chnage in HF was observed for any site of Fe in Fe_3B. This means that Co does not go to Fe_3B crystal, rather the Co partitions to $Nd_2Fe_{14}B$ as was suggested already by examining the change of lattice parameters. Eventually a prominent decrease in HF for $8j_2$ site in $Nd_2Fe_{14}B$ was observed. Since the number of nearest neighbor Fe atoms is 12 in $Nd_2Fe_{14}B$ crystal, the probability of Co substitution for Fe is high at the $8j_2$ site compared with the other sites. Likewise a slight decrease in HF for 4c site, where the number of nearest Nd is 4, was observed. Since the attraction force of Co with Nd is rather higher than that with Fe, Co tends to partition to 4c site rather than 4e site which results in a decrease in HF with the addition of Co.

4. Conclusion

The addition of Co into $Nd_4Fe_{77.5-x}Co_xHf_{0.5}Ga_{0.5}B_{18.5}$($0 \leq x \leq 5$) was found to enhance the magnetic properties of $Fe_3B/Nd_2Fe_{14}B$ nanocomposite magnets. The enhancement resulted from the fact that Co tends to retard the formation of Fe_3B from the amorphous matrix but accelerate that of $Nd_2Fe_{14}B$. The decreased interval between the crystallization temperature of Fe_3B and $Nd_2Fe_{14}B$ led to a uniform grain size distribution of the both phases during the annealing treatment. The additive Co was confirmed to partition mainly to $Nd_2Fe_{14}B$ crystals rather than to Fe_3B which was traced by XRD and Mossbauer spectroscopy as well. About 72 vol.% of Fe_3B, 27 vol.% of $Nd_2Fe_{14}B$, and small amount of Fe around 1 vol.%, respectively, were found to form. However, The volume fraction of each phase was not to vary by the addition of Co up to 5 at.%.

References

[1] C. J. Yang and E. B. Park, J. Magn. Magn. Mater., **166**, 243 (1997).

[2] S. Chikazumi, in "Physics of Magnetism", John-Wiley and Sons, New York, 554 (1964).

[3] J. F. Herbst, R. W. Lee and F. E. Finkerton, Annu. Rev. Mater. Sci., **16**, 467 (1986).

[4] R. Yapp and H. A. Davis, in Proc. of The 15th Inter. Workshop on Rare Earth Magnets and Their Applications, Aug. 30-Sept. 4, Dresden, Germany, 315 (1998).

[5] Gao Youhui, J. H. Zhu, C. J. Yang and E. B. Park, J. Magn. Magn. Mater., **186**, 97 (1998).

[6] D. H. Ping, K. Hono and S. Hirosawa, J. Appl. Phys., **83**(12), 7769 (1998).